EurJIC
European Journal of Inorganic Chemistry

Research Article
doi.org/10.1002/ejic.202100939

Chemistry Europe
European Chemical Societies Publishing

www.eurjic.org

Synthesis, Structure and Cu-Phenylacetylide Coordination of an Unsymmetrically Substituted Bulky dppf-Analog

Subhayan Dey,[a] Fabian Roesler,[a] Mark V. Höfler,[b] Clemens Bruhn,[a] Torsten Gutmann,*[b] and Rudolf Pietschnig*[a]

The donor properties of a set of bulky ferrocene based bisphosphanes ($Fe(C_5H_4PMes_2)_2$ and $(C_5H_4PMes_2)Fe(C_5H_4P^tBu_2$ with Mes = mesityl and ^{t}Bu = *tert*-butyl) were probed by exploring the NMR parameters of the corresponding selenophosphoranes amended by cyclovoltammetry. The ligand properties were explored in the complexation of copper phenylacetylide which is relevant as intermediate in the Cu(I) catalyzed CO_2 addition to phenylacetylene. Owing to the poor solubility of the resulting complexes their characterization was performed with solid state NMR spectroscopy amended by IR spectroscopy, mass spectrometry and elemental analysis. Remarkably, these complexes feature luminescent properties, albeit with limited quantum yield.

Introduction

Ferrocenyl bisphosphanes are an important ligand scaffold, not only for their hassle-free modular syntheses and easy modification, but also for their ability to form complexes with a wide variety of metal ions, via facile geometric adaptation.[1] By changing the steric bulk at the phosphorus donor centers and altering the metal cations, many different complexation motifs have been explored for these compounds, such as, 'classical chelate' (Figure 1A), 'open-bridge' (Figure 1B), 'quasi-closed bridge' (Figure 1C), 'double-bridge' (Figure 1D), 'η^1, η^1-intra-bridge' (Figure 1E), 'η^1, η^1-interbridge' (Figure 1F), and 'quasi-closed double-bridged' complexes (Figure 1G).[1b,c,2] Although most of the above-mentioned patterns are known for years,[2a] other bonding motifs, like the 'quasi-closed double-bridged' arrangement (Figure 1G) emerged only recently and are controlled by optimal steric bulk.[1a,2b]

Although many different 1,1′-symmetrically and unsymmetrically substituted bisphosphanoferrocenes have been reported in literature,[6] catalytic applications focused on 1,1′-bis(diphenylphosphano)ferrocene (dppf) for many decades.[1b,7] Higher steric bulk on phosphorus centers generally result in higher bite angles and sometimes increased catalytic activity according to experimental,[1a,8] as well as theoretical studies.[9] To increase steric bulk on the phosphorus centers of dppf-analogs and to test the steric tolerance for catalysis, our group has recently introduced mesityl group on phosphorus centers. During investigation of the CO_2-addition to terminal alkynes catalyzed by copper complexes of such bisphosphanes, it was found that the symmetrically substituted tetramesityl species **1** is prone to fragmented complexation and therefore, shows poor catalytic yield.[2b] Generally, in situ formed Cu-acetylide complexes are central intermediates in the above mentioned reaction based on quantum chemical studies.[2b]

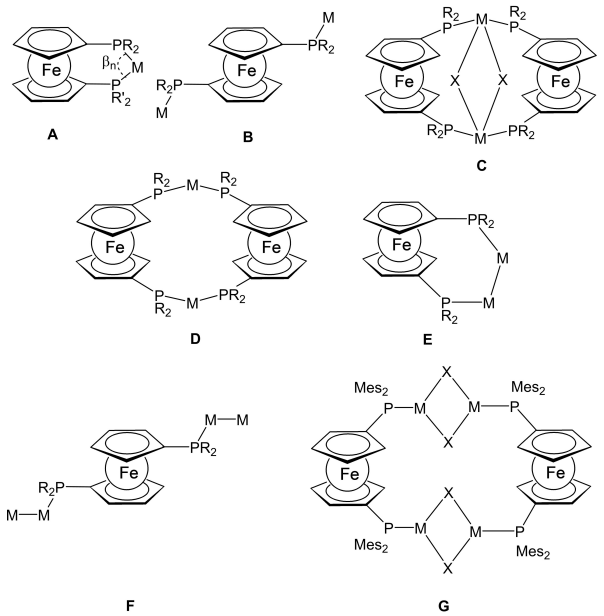

Figure 1. Different complexation motifs of dppf-analogs [R = Ph, R′ = tBu and M = PdCl2 for **A**;[3] R = Ph and M = ClMn(CO)4 for **B**;[4] R = Ph and MX = $AgNO_3$ for **C**;[5] R = Ph and M = Ag for **D**, **E** and **F**;[5] MX = CuBr for **G**].[1a,2b]

[a] *Dr. S. Dey, Dr. F. Roesler, Dr. C. Bruhn, Prof. Dr. R. Pietschnig*
Institute for Chemistry and CINSaT, University of Kassel,
Heinrich Plett-Straße 40, 34132 Kassel, Germany
E-mail: pietschnig@uni-kassel.de
https://www.uni-kassel.de/go/hym
[b] *M. V. Höfler, Dr. T. Gutmann*
Technical University Darmstadt,
Eduard Zintl-Institute for Inorganic and Physical Chemistry,
Alarich-Weiss-Straße 8, 64287 Darmstadt, Germany
E-mail: gutmann@chemie.tu-darmstadt.de
https://www.chemie.tu-darmstadt.de/gutmann/rg_gutmann/index.en.jsp

Supporting information for this article is available on the WWW under https://doi.org/10.1002/ejic.202100939

Part of the "Ferrocene Chemistry" Special Collection.

Research Article
doi.org/10.1002/ejic.202100939

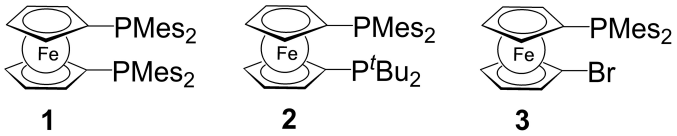

Figure 2. Mono- and disubstituted ferrocene based phosphane ligands under investigation.

In the present study, we explore the nature of such Cu-acetylide complexes of the previously reported tetramesityl substituted dppf-analog **1**, and related sterically demanding mixed species **2** and **3**, where apart from two mesityl units, two *tert*-butyl units are attached to the phosphane donor centers (Figure 2). For these ligands we have further explored their redox properties with cyclic voltammetry and their donor properties via NMR spectroscopy of the corresponding selenophosphorane derivatives. Given the interest currently devoted to the luminescence properties of Cu(I)-complexes,[10] we also explore this aspect in our investigation.

Results and Discussion

Syntheses and Comparison of 1–3

The unsymmetrically substituted bisphosphano ligand **2** was synthesized by following a published approach, used for its dimesityl and diphenyl counterpart Fc′(PMes$_2$)(PPh$_2$).[2b] As depicted in Scheme 1, when compound **3** was first selectively monolithiated and subsequently in situ reacted with ^{t}Bu$_2$PCl, compound **2** was obtained in a yield of ~60 %. After purification via crystallization, compound **2** was further reacted with red selenium, to obtain the selenophosphorane species **4** (Scheme 1).

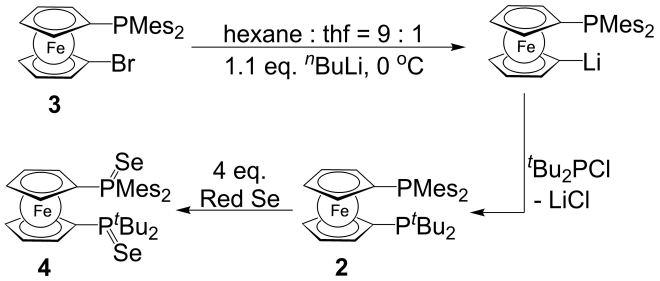

Scheme 1. Schematic presentation of the synthesis of compounds **2** and **4**.

Species **4** has further given us the opportunity to compare the electron donating ability of ^{t}Bu-substituted phosphorus centers with that of its mesityl- and phenyl-substituted counterparts.[11] Since the NMR data of the selenide of its all mesityl-substituted counterpart (Figure 3A) have been reported in toluene-D8, similar measurements of compound **4** were also performed in the same solvent. Here, it should be noted that $^1J_{P–Se}$, the key component to determine the relative *s*- and *p*-contributions of the underlying phosphorus lone pair and the nature of the P–Se σ-bond,[1a] is highly solvent dependent. For example, the selenide of dppf (Figure 3B) shows the $^1J_{P–Se}$ coupling values 761 and 737 Hz in toluene-D8 and $CDCl_3$, respectively.[1a] Therefore, closely related compounds are difficult to compare unless their reported data have been recorded in the same solvent [e.g. $^1J_{P–Se}$ for Fc(PSe^{t}Bu$_2$), measured in $CDCl_3$, 702 Hz].[12] Nevertheless, the trend of decreasing $^1J_{P–Se}$ values, with increasing steric congestion has been observed for various phenyl and *tert*-butyl-substituted PSeR$_3$ compounds: $^1J_{P–Se}$ for PSePh$_3$, PSe(*o*-Tol)$_3$, PSe(*m*-Tol)$_3$, PSe(*p*-Tol)$_3$, PSe(C$_6$H$_4$-

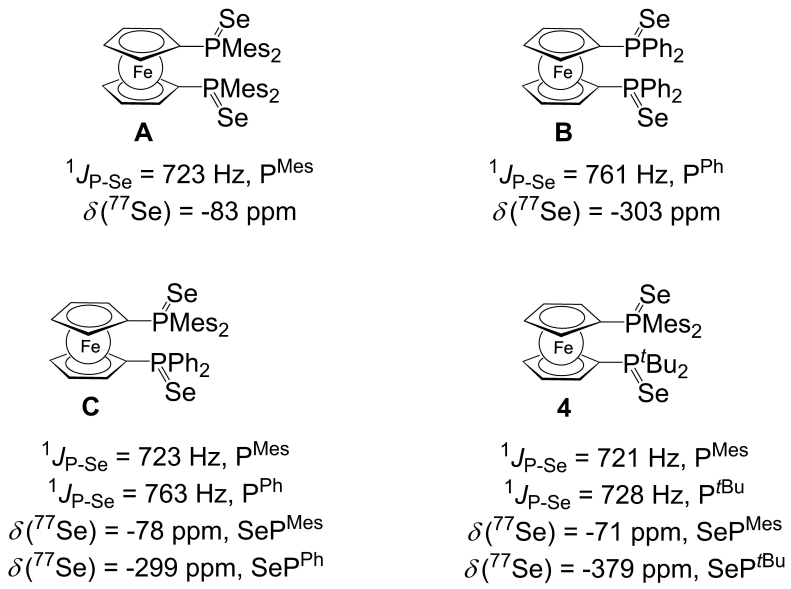

Figure 3. ^{31}P- and ^{77}Se NMR parameters (measured in toluene-D8) related to selenides of sterically bulky dppf-analogs.

Research Article
doi.org/10.1002/ejic.202100939

p-OMe)$_3$, and PSe(*o*-Tol)$_2$Ph, measured in $CDCl_3$, are 730–737, 708, 726, 724, 719, and 730 Hz, respectively; and $^1J_{P-Se}$ for PSe^{t}Bu$_3$, measured in C_6D_6 and CD_2Cl_2, are 709 and 693 Hz, respectively.[2b,11a, 12b, 13] It should be mentioned here that trends in $^1J_{P-Se}$ do not always correlate with other ligand parameters, such as TEP values (Tolman's electronic parameter), corresponding to the vibrational frequency of the carbonyl symmetric stretching mode of [Ni(CO)$_3$L] complexes), as the electronic parameter for these ligands often runs in opposite to their steric parameter. For example, the $^1J_{P-Se}$ values for PSeMe$_3$ ($^1J_{P-Se}$ = 682 Hz in $CDCl_3$),[14] PSePh$_3$ ($^1J_{P-Se}$ = 737 Hz in $CDCl_3$),[2b] and PSe^{t}Bu$_3$ ($^1J_{P-Se}$ = 693 Hz in CD_2Cl_2),[13c] indicate that the electron donating ability of the corresponding P centers follow a trend of PMe$_3$ > P^{t}Bu$_3$ > PPh$_3$, whereas for steric reasons, the availability of the lone pair follows the trend of PMe$_3$ > PPh$_3$ > P^{t}Bu$_3$.[15] Therefore, a linear relation between $^1J_{P-Se}$ and Tolman's electronic parameter is difficult to draw.

The $^1J_{P-Se}$ for both the phosphorus centers in compound **4** (721 and 728 Hz, Figure 3) is significantly lower than the corresponding values for Ph$_2$P[Se] in dppf[Se]$_2$ (761 Hz for **B**, Figure 3),[2b] and Fc′(PSeMes$_2$)(PSePh$_2$) (763 Hz for **C**, Figure 3),[2b] which indicates that the lone pairs of both phosphorus atoms in **2** have significantly lower *s* character, and therefore, higher donating ability than phenyl-substituted ferrocenyl phosphines. On the other hand, the mesityl-substituted phosphorus center in **4** has a slightly lower $^1J_{P-Se}$ value (for ca. 7 Hz) than its *tert*-butyl-substituted counterpart, which means that former (Mes-substituted P) has a lower *s* character and higher donating ability than the latter (^{t}Bu-substituted P). A similar trend could also be noticed for the ^{77}Se NMR chemical shift of **4**, where the resonance of Mes$_2$P[Se] at δ −71.1 ppm is deshielded by ca. δ 308 and 230 ppm, compared to ^{t}Bu$_2$P[Se] (in **4**, see Figure S8 in ESI file), and Ph$_2$P[Se] units (in **C**), respectively.[2b] These features indicate a comparable dative P–Se interaction for PMes$_2$ and P^{t}Bu$_2$ units in agreement with the NMR data outlined above, whereas the sterically less hindered phosphane unit, like PPh$_2$, results in larger $^1J_{P-Se}$ coupling values and stronger shielding of the ^{77}Se resonance (δ −303 and −299 ppm for **B** and **C**, respectively) in the corresponding selenophosphorane. Combining all these above-mentioned data, the following trend can be concluded, regarding p-character and donating ability of lone pairs: Mes$_2$P ≥ ^{t}Bu$_2$P > Ph$_2$P, where ≥ and > signs have been used to indicate the relative value for the corresponding parameter.

To explore the overall electronic effect of replacing mesityl with *tert*-butyl units in this molecular scaffold, the redox properties of these metallocene units have been investigated using cyclic voltammetry (CV). The redox cycle of compound **2** is quasi-reversible in nature, and the oxidation reaction occurs at 0.31 V (see Figure S22 in ESI file), which is shifted to higher potentials in comparison to those of dppf (E° = 0.18 V),[1a] all-mesityl substituted analog Fc′(PMes$_2$)$_2$ (**1**, E° = 0.13 V),[2b] and mixed species Fc′(PMes$_2$)(PPh$_2$) (E° = 0.16 V).[2b] The results obtained from cyclic voltammetry indicate an electronic scenario, in which the electron density at the ferrocene unit follows the trend of **1** > dppf > **2**. In contrast to the present results, no anodic but a cathodic shift of dppf-analogs was observed when phenyl groups in dppf were replaced with more electron-donating *tert*-butyl or mesityl units, as for instance in Fc′(PPh$_2$)(P^{t}Bu$_2$) (E° = 0.11 V) and Fc′(P^{t}Bu$_2$)$_2$ (E° = 0.06 V), or Fc′(PMes$_2$)(PPh$_2$) (E° = 0.16 V) and Fc′(PMes$_2$)$_2$ (E° = 0.13 V), respectively.[1a] This corroborates that the substitution pattern at phosphorus affects the electronic situation at the metallocene unit. However, in turn no clear connection between redox potentials of the metallocene unit and the donor properties of the adjacent lone pair at phosphorus can be derived. Moreover, the HOMO may be either iron centered or phosphorus centered,[16] or further be complicated by dynamic electron transfer processes.[17] The non-reversible redox properties of **1**, contrasting the reversible redox behavior of **2**,[2b] may be interpreted as indication for an energetically relatively high lying lone pair at phosphorus in **1**, for which better donor properties may be anticipated, owing to its increased higher p-character. In agreement with this, the $^1J_{P-Se}$ values derived from NMR measurements as discussed above directly reveal the properties of the respective phosphorus donor atoms following the trend of **1** ≥ **2** > dppf, similarly highlighting ligand **1** as the strongest donor in this sequence.

Suitable single crystals for X-ray analyses were obtained for compounds **1**, **2**, and **4**. While Figure 4, Figure 5, and Figure 6 show the molecular structures of **1**, **2** and **4** respectively, their refinement data are listed in Table S1 (ESI file). The molecular structures of **1** and **2** in the solid state show a sum of angles of 311.1(9)° and 315.23(44)°, respectively at the phosphorus atoms of the PMes$_2$ units, which are similar to the respective value for the P^{t}Bu$_2$ unit in molecule **2** (313.14(50)°), indicating comparable steric interaction in both the phosphorus centers. On the other hand, both of these values are considerably higher than that of the PPh$_2$ unit in **C** (303.37(16)°),[2b] indicating substan-

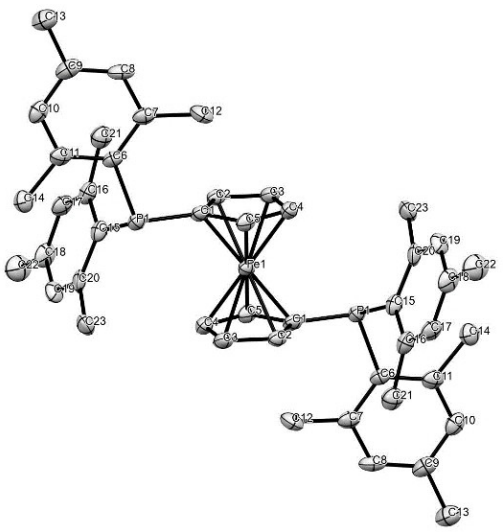

Figure 4. Ortep plots of the molecular structures of **1** in the solid state with ellipsoids drawn at the 50% probability level. Labels for some selected atoms, solvent molecules and H atoms are omitted for clarity. Selected bond lengths [Å] and angles [°]: P(1)-C(1) 1.833(7), P(1)-C(6) 1.857(7), C(1)-P(1)-C(15) 99.5(3), C(1)-P(1)-C(6) 108.9(3), C(15)-P(1)-C(6) 102.7(3). Further details can be found in Tables S2 and S3 in ESI file.

Research Article
doi.org/10.1002/ejic.202100939

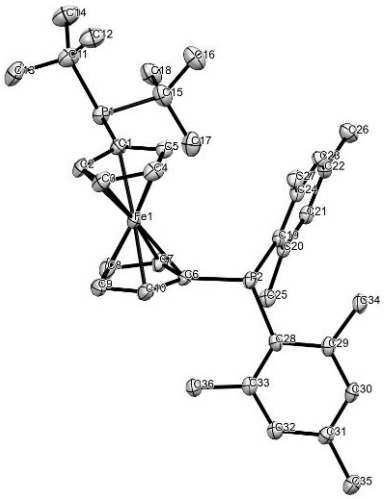

Figure 5. Ortep plots of the molecular structures of **2** in the solid state with ellipsoids drawn at the 50% probability level. Labels for some selected atoms, solvent molecules and H atoms are omitted for clarity. Selected bond lengths [Å] and angles [°]: P(2)-C(6) 1.809(3), P(2)-C(19) 1.848(3), P(1)-C(1) 1.843(3), P(1)-C(15) 1.897(4), P(1)-C(11) 1.917(4), C(1)-P(1)-C(11) 98.91(16), C(1)-P(1)-C(15) 105.15(16), C(15)-P(1)-C(11) 109.08(18), C(5)-C(1)-P(1) 133.3(3), C(2)-C(1)-P(1) 119.5(3), C(12)-C(11)-P(1) 114.7(3), C(6)-P(2)-C(19) 102.05(15), C(6)-P(2)-C(28) 109.52(15), C(19)-P(2)-C(28) 103.66(14). Further details can be found in Tables S4 and S5 in ESI file.

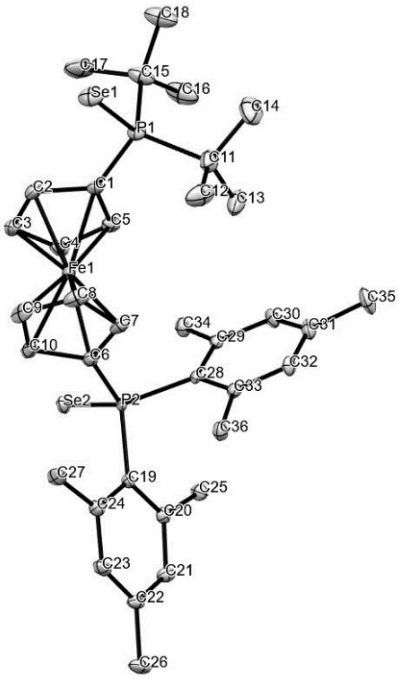

Figure 6. Ortep plots of the molecular structures of **4** in the solid state with ellipsoids drawn at the 50% probability level. Labels for some selected atoms, solvent molecules and H atoms are omitted for clarity. Selected bond lengths [Å] and angles [°]: C(1)-P(1) 1.804(4), Se(1)-P(1) 2.1312(11), P(1)-C(11) 1.873(5), P(2)-C(6) 1.808(4), Se(2)-P(2) 2.1344(10), P(2)-C(28) 1.837(4), C(1)-P(1)-Se(1) 111.65(14), C(1)-P(1)-C(11) 110.4(2), C(1)-P(1)-C(15) 100.7(2), C(11)-P(1)-Se(1) 111.00(18), C(11)-P(1)-C(15) 113.6(2), C(15)-P(1)-Se(1) 109.08(16), C(6)-P(2)-Se(2) 108.30(14), C(6)-P(2)-C(19) 114.59(19), C(6)-P(2)-C(28) 101.08(18), C(19)-P(2)-Se(2) 104.39(13), C(19)-P(2)-C(28) 105.09(17), C(28)-P(2)-Se(2) 123.87(13), C(28)-C(29)-C(34) 124.7(3). Further details can be found in Tables S6 and S7 in ESI file.

tially higher steric congestion compared with the diphenylphosphanyl unit.

Similar trends can also be observed when the crystallographic structures of selenophosphoranes **A**, **C** and **4**, are compared. By careful evaluation of their structures, it can be found that the sum of C–P–C angles around P[Se]Mes_2 units are in a range of 319°–322° (319.45(30)°,[2b] 321.8(6)°,[2b] and 320.76(54)° for **A**, **C** and **4**, respectively, which is almost identical to the corresponding values for P[Se]^tBu_2 unit in **4** (324.7(6)°), and higher than the similar value for P[Se]Ph_2 unit in **C** (315.2(6)°).[2b] Consistent with these findings, the P–Se bond lengths are comparable for P[Se]Mes_2 (2.1312(11) Å) and P[Se]^tBu_2 (2.1344(10) Å) units, but higher than the corresponding value for P[Se]Ph_2 unit in **C** (2.0971(13) Å). Combining all these above-mentioned data, the following trend can be concluded, regarding steric demand on phosphorus centers: $Mes_2P \approx {}^tBu_2P > Ph_2P$, where $\approx$ and $>$ signs have been used to indicate the relative value for the corresponding parameter.

Complexation of 1–3

To explore the ligand properties towards d-block metals and in order to compare such complexes with reported results,[2b,18] [Cu(C≡C–Ph)]-complexes **5**–**7** were synthesized from ligands **1**–**3**, using a common synthetic methodology (Scheme 2). As these complexes have very poor solubility in common organic solvents, they have been characterized with solid-state characterization methodologies, such as, solid-state NMR and IR, MALDI, elemental analyses and solid-state UV-Vis spectrometry. Owing to the polymeric nature of copper acetylides, and fragmented complexation motif of $PMes_2$ units, we speculate that [Cu(C≡C–Ph)]-complexes **5**–**7** exists as clusters like **D**, rather than being oligomers like **E** and **F** (Scheme 2). Low solubility of these complexes and their photo-luminating behavior,[10w,18c,19] also indicate their aggregated arrangement.

$^1H \rightarrow {}^{13}C$ CP MAS spectra of complexes 5–7

All spectra (Figures S13–S15, ESI file) show a couple of signals in the region between δ 120–150 ppm, which can be attributed to the aromatic system in mesityl groups. Additionally, a couple of signals appear in the region between δ 60–85 ppm, which are typical for carbon resonances in the cyclopentadienyl rings of the ferrocene unit. Moreover, all samples show signals between δ 20–30 ppm, which can be attributed to the methyl groups present in the mesityl moieties. Complex **6** shows additional signals between δ 30–35 ppm, which indicate the presence of ^{t}Bu groups. In agreement with the proposed structures, these signals are not visible in the other samples.

Research Article
doi.org/10.1002/ejic.202100939

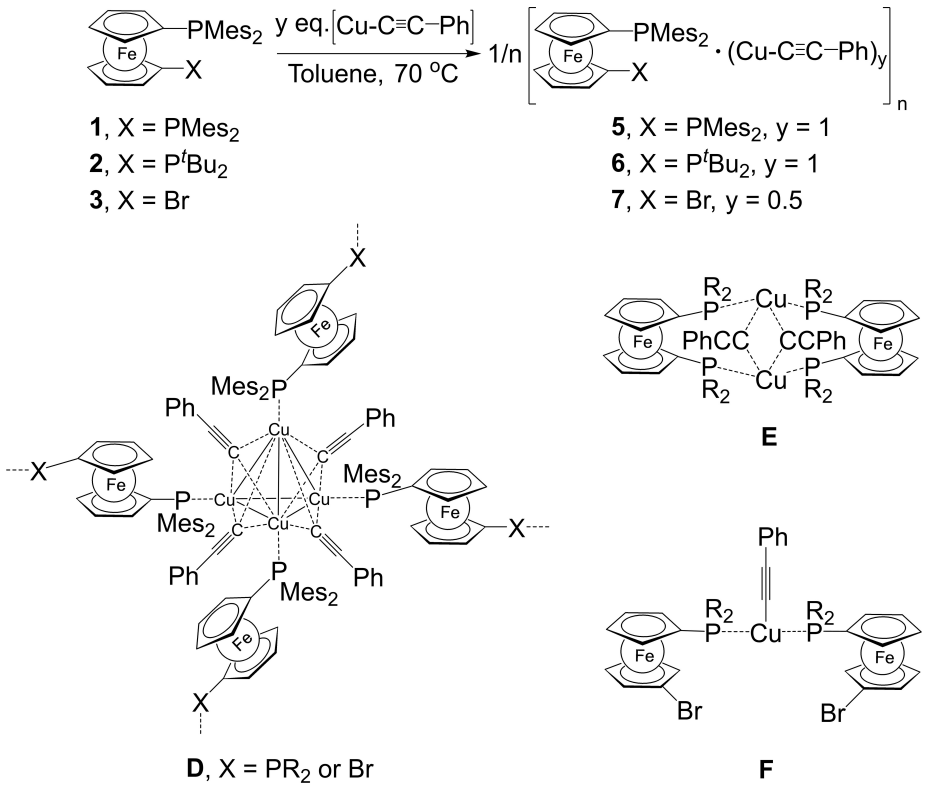

Scheme 2. [Cu(C≡C–Ph)]-complexes of **1**, **2** and **3**. The possible structures of oligomeric and polymeric moieties have been inspired by $[Cu_2(\mu\text{-}\eta^1\text{-}C{\equiv}C{-}C_6H_4\text{-}4\text{-}CH_3)_2(\mu\text{-dppf})_2]$,[18a] $[Fc'(P^tBu_2)_2{\cdot}CuCN]_2$,[20] and $[CuPPh_3\text{-}\mu_3\text{-}C{\equiv}C{-}Ph]_4$,[18d] $[Cu_3(dppm)_3(\mu_3\text{-}\eta^1\text{-}C{\equiv}C\text{-}{}^tBu)_2]$,[18e] respectively.

$^1H{\rightarrow}^{31}P$ CP MAS spectra of complexes 5–7

Complex **5** shows a signal at δ −36 ppm (Figures S16, ESI file), which relies to the phosphorus, connected to the mesityl groups. On the other hand, complex **6** shows two signals in the ^{31}P spectra (Figure S17, ESI file): the signals at δ 23 and −39 ppm can be attributed to the phosphorus atoms, connected to the *tert*-butyl and mesityl-groups, respectively. Complex **7** shows two resonances at δ −36 and −38 ppm (Figure S18, ESI file), which is quite unexpected, since the structure shows only one possible P–Cu coordination. However, it is feasible that this is an effect of the solid-state measurement, where typically the phosphorus nuclei in these compounds may become magnetically inequivalent, due to the surrounding topology.[21] To verify this hypothesis, more sophisticated solid state NMR experiments are required which are beyond the scope of the present work.

UV-Vis Spectroscopy of complexes 5–7

Interestingly the investigated complexes **5**–**7** are luminescent despite the presence of ferrocene units, which are known for their intramolecular luminescence quenching properties.[22] The compounds show an absorption maximum between 384 and 450 nm in solid state (Figure S23, ESI file). The corresponding emission maxima are almost identical (511–513 nm) and the quantum yields vary from 0.6 to 1.1 %. For comparison the used educt, copper phenylacetylide was also investigated. In the absorption spectrum, the maximum is red shifted towards 472 nm. Similarly, a bathochromic shift was observed in the emission maximum which is located at 524 nm with a quantum yield of 1.3 %. Although the quantum yield is very limited compared with other luminescent Cu(I)-complexes (e.g. quantum yields of selected complexes at room temperature and in solid state are enlisted as follows: $Cu_4I_4(PPh_3)_4$ (44 %),[10u] $[Cu_2(dcpm)_2(CH_3CN)_2](BF_4)_2$ (26 %),[10y] $[Cu_2(dcpm)_2](BF_4)_2$ (42 %),[10y] $[(CuI)_3(dcpm)_2]$ (11 %),[10y] $[(Trip\text{-}C{\equiv}C)Cu]_8$ (21 %)],[10z] where dcpm and Trip stand for bis(dicyclohexylphosphano)methane and 2,4,6-triisopropylphenyl, respectively], it is nevertheless remarkable for a ferrocene-based complex, as reports on luminescent ferrocene complexes with transition metals are extremely rare.[2a,23]

Conclusion

In summary, the dimesityl- and di-*tert*-butyl-substituted analogue of dppf, **2** has been synthesized and its ligand properties explored. The phosphorus lone pair of dimesityl-substituted center of **2** shows a similar *s* character, and therefore, a comparable donating ability to that of di-*tert*-butyl-substituted one, as indicated by spectroscopic and structural means. However, the comparison of compound **2** and **1** with cyclic

Research Article
doi.org/10.1002/ejic.202100939

voltammetry showed a substantial anodic shift of the Fc/Fc^+ oxidation of **2** indicating lower electronic density at iron than in **1**. Similarly, the $^1J_{P-Se}$ coupling of the corresponding selenophosphoranes corroborate the superior donor properties of **1** referring directly to the phosphorus donor units. The complexation of ligands **1**–**3** with copper phenylacetylide resulted in insoluble species which have been characterized by solid-state spectroscopic techniques and elemental analyses. Moreover, these complexes feature luminescent properties which is remarkable for ferrocene compounds, albeit with limited quantum yield. The potential of bulky dppf-analog **2** for complexation with other metals and the catalytic activity of resulting complexes will be explored in the near future.

Experimental Section

All manipulations were performed under argon atmosphere unless mentioned otherwise. Prior to use, the glassware was dried in drying oven under 120 °C. Solvents were distilled over drying agents, prescribed in CRC Handbook of chemistry and subsequently stored under argon atmosphere over 4 Å molecular sieves. Solvents for column chromatography and aqueous workups were used from bottle (analytical grade supplied by VWR and Alfa-Aesar) without further purification. NMR solvents (purchased from Deutero) were degassed via a few cycles of freeze, pump and thaw, and finally stored over 3 Å molecular sieves under argon atmosphere. Reagents and chemicals were purchased from commercial suppliers (Sigma-Aldrich, ABCR, Alfa-Aesar) and used as received. $Fc'(PMes_2)_2$ (**1**), $Fc'(PMes_2)_2Br$ (**3**) and Cu(C≡CPh) were synthesized by following the reported procedure.[2b,24] Due to minor side reactions, such as, unwanted dilithiation and subsequent in situ hydrolysis, compound $Fc'(PMes_2)(P^tBu_2)$ contains an impurity, where only one dimesitylphosphano group is present on ferrocene. We could not remove this compound from the targeted species which was, therefore, contaminated with ca. 4% of dimesitylphosphanoferrocene for the next chemical transformations.

All solution-phase NMR spectra were measured with Varian 500V NMRS and Varian MR-400 spectrometers at 22 °C. Chemical shifts (δ in ppm) were expressed with respect to the following standards, set as 0 ppm: $SiMe_4$ (for ^1H and ^{13}C), aqueous H_3PO_4 (for ^{31}P), $BF_3{\cdot}OEt_2$ (in $CDCl_3$ for ^{11}B) and $CFCl_3$ (for ^{19}F). The signals, resulting from the residual nondeuterated NMR solvents, were referenced as indicated in the literature.[25] In addition to the standard notation of the signal multiplicity (s = singlet, d = doublet, m = multiplet, dd = doublet of doublet etc.), pst, brs, brd and brm were used to abbreviate pseudotriplet, broad singlet, broad doublet and broad multiplet, respectively in order. The amount of residual solvents (if present) was verified by NMR analysis and the expected values for elemental analyses were calculated accordingly.

All solid-state NMR measurements were performed on a Bruker Avance III HD 300 MHz spectrometer employing a 4 mm broad band H/X probe. Samples were packed into 4 mm ZrO_2 rotors. All spectra were recorded at 7 T, which leads to a frequency of 75.47 MHz for ^{13}C and 121.49 MHz for ^{31}P, at room temperature with a MAS spinning frequency of 8 kHz. The CP MAS sequence was used with a linear ramp on ^1H and contact times of 3 ms for ^{13}C and 3.2 ms for ^{31}P. The acquisition time for $^1H{\rightarrow}^{13}C$ and for $^1H{\rightarrow}^{31}P$ CP MAS experiments was set to 25 ms and a TPPM15 broadband decoupling was applied during data acquisition.[26] A recycle delay of 1 s was used for all spectra. ^{13}C spectra were recorded with 5120 scans and ^{31}P spectra were recorded with 2048 scans. As a reference H_3PO_4 (δ 0 ppm) was used for ^{31}P and TMS (δ 0 ppm) for ^{13}C employing adamantane as an external standard.

When Electrospray ionization (ESI) and Atmospheric pressure chemical ionization (APCI) mass spectra were measured with a Finnigan LCQ Deca (ThermoQuest, San Jose, USA) instrument using samples dissolved in HPLC-quality thf, MALDI was measured with an UltraFlex ToF/ToF (Bruker Daltonics, Bremen, D) instrument, where an N_2 laser with 337 nm wavelength and 3 ns pulse duration was used. Elemental analyses were performed without the presence of any external oxidizer (like V_2O_5) in an EA 3000 Elemental Analyzer (EuroVector). The values of elemental analyses, reported in this article is actually the average of three consecutive readings taken from the purest specimens of each compound. X-ray diffraction experiments were performed using a STOE StadiVari [using either Mo-GENIX source (λ = 0.71073 Å), or Cu-GENIX source (λ = 1.54186 Å)] diffractometer. Structures were solved using dual space method (SHELXT) and were refined with SHELXL-2018.[27] All non-hydrogen atoms were refined anisotropically, whereas hydrogen atoms were placed on adjacent atoms using a riding model. Further programs used in the structure analyses were Mercury and Platon.[28] CCDC-2119544-2119546 contain the supplementary crystallographic data for this paper. These data can be obtained free of charge from The Cambridge Crystallographic Data Centre via www.ccdc.cam.ac.uk/data_request/cif.

Absorption and emission spectra, as well as luminescence quantum yields (absolute method), were measured with the Hamamatsu C11347 system in solid state and for the refinement of data, OriginPro was used. CV measurement was done with GB2202-C-VAC under Argon atmosphere, when samples were measured as a solution (1 mM) in dry and deoxygenated CH_2Cl_2, where anhydrous $[Bu_4N][PF_6]$ was used as a conducting salt at a concentration of 0.1 M. The three-electrode cell consisted of a platinum working electrode, a silver counter electrode, and a silver pseudo reference electrode. The potential was driven on a WaveDriver 20 Bipotentiostat from Pine Research Instrument, and the electrochemical data was recorded via AfterMath (Ver. 1.5.9807, Pine Instrument). All the redox processes were referenced using half-wave potentials of $FcMe_{10}$ as a standard, which was added to the analysed solution. Its corresponding value was then subtracted from the recorded potentials to convert them to the Fc/Fc^+ scale following established procedures,[29] and finally evaluated with AfterMath and OriginPro.

$Fc'(PMes_2)(P^tBu_2)$ (2)

^{n}BuLi (2.5Min hexanes, 0.17 mL, 0.43 mmol) was added dropwise to a cold (0 °C) thf (20 mL) solution of $Fc'(PMes_2)Br$ (0.200 g, 0.38 mmol). After the gradual color change from orange to bright red, the solution was stirred at 0 °C for 30 min. Another solution of $^tBu_2PCl$ (85 µL, 0.081 g, 0.45 mmol) in hexanes (10 mL) was slowly added to the above cold solution over 5 min. After warming up to the ambient temperature, the reaction mixture was stirred overnight. All volatiles were removed under high vacuum (10–3 mbar) and the product was extracted with hexanes (20 mL). The volume of the filtrate was reduced to ca. 5 mL and the almost pure compound was obtained as yellow crystals (62%) upon refrigeration at −78 °C. NOTE: This product had an impurity of dimesitylphosphanoferrocene (ca. 2–3%) which could not be reduced upon further crystallization. ^1H NMR (toluene-d8): δ 1.12 (d, 18H, ^{t}Bu, J = 11 Hz), 2.10 (s, 6H, *p*-CH3 of Mes), 2.36 (s, 12H, *o*-CH_3 of Mes), 4.12 (pst, 2H, β-H of CpP^{tBu2}), 4.20 (pst, 2H, α-H of $CpCpP^{tBu2}$), 4.25 (pst, 2H, β-H of Cp^{PMes2}), 4.26 (pst, 2H, α-H of Cp^{PMes2}), 6.69 (brd, 4H, m-H of Mes, J = 2 Hz). ^{13}C NMR (toluene-d8): δ 20.86 (s, *p*-CH_3 of Mes), 23.54 (d, *o*-CH_3 of Mes, J = 15 Hz), 31.01 (d, $C(CH_3)_3$, J = 14 Hz), 32.72 (d, $C(CH_3)_3$, J = 23 Hz), 71.09 (d, β-C of Cp^{PMes2}, J = 3 Hz), 72.62 (d, β-C

of Cp^{PtBu2}, $J = 4$ Hz), 74.55 (d, α-C of Cp^{PMes2}, $J = 13$ Hz), 76.51 (d, α-C of Cp^{PtBu2}, $J = 18$ Hz), 80.03 (d, *ipso*-C of Cp^{PMes2}, $J = 2$ Hz), 80.26 (d, *ipso*-C of CpP^{PtBu2}, $J = 19$ Hz), 130.51 (d, *p*-Aryl C of Ph, $J = 3$ Hz), 132.77 (d, *ipso*-C of Ph, $J = 21$ Hz), 137.55 (d, *m*-Aryl C of Ph), 142.57 (d, *o*-Aryl C of Ph, $J = 15$ Hz). ^{31}P NMR (toluene-d8): δ −34.7 (s, $PMes_2$), 26.8 (m, P^tBu_2). MS (APCI-DIP): m/z (%) 599 (100) $[M]^+$. HRMS (APCI-DIP; m/z): $[M+1]^+$ calc for $C_{36}H_{49}FeP_2$, 599.25807; found 599.26540. Anal. Calcd. for $C_{36}H_{48}FeP_2$: C, 72.24; H, 8.08. Found: C 72.39; H, 8.17.

Fc′(PSeMes$_2$)(PSe^{t}Bu$_2$) (4)

A suspension of red Se (0.120 g, 1.52 mmol) and **2** (0.144 g, 0.24 mmol) in thf (20 mL) was stirred for 1 hr at r.t. All the volatiles were removed under high vacuum (10^{-3} mbar) and the product was extracted with hot toluene. Analytically pure compound was crystallized from the hot toluene solution by slow cooling up to ambient temperature. NOTE: If all the residual Se is not removed by single filtration attempt, the procedure of filtration must be repeated for multiple times before crystallization. Yield: 85 %. ^{1}H NMR (toluene-d8): δ 1.14 (d, 18H, C(CH_3)$_3$ of ^{t}Bu), 2.00 (m, 6H, *p*-CH_3 of Mes), 2.40 (brs, 12H, *o*-CH_3 of Mes), 4.44 (m, 2H, β-H of Cp^{PtBu2}), 4.70 (m, 2H, β-H of Cp^{PMes2}), 4.80 (brs, 2H, α-H of Cp^{PMes2}), 4.89 (m, 2H, α-H of Cp^{PtBu2}), 6.52 (brd, 4H, *m*-H of Mes, $J = 4$ Hz). ^{13}C NMR (toluene-d8): δ 20.67 (d, *p*-CH_3 of Mes, $J = 2$ Hz), 24.36 (d, *o*-CH_3 of Mes, $J = 5.9$ Hz), 28.70 (d, C(CH_3)$_3$, $J = 2.2$ Hz), 38.05 (d, $C(CH_3)_3$, $J = 36.5$ Hz), 74.50 (d, β-C of $Cp^{PSetBu2}$, $J = 7.9$ Hz), 75.31 (d, β-C of $Cp^{PSeMes2}$, $J = 8.8$ Hz), 75.82 (d, α-C of $Cp^{PSetBu2}$, $J = 9.3$ Hz), 76.67 (d, *ipso*-C of $Cp^{PSetBu2}$, $J = 60.6$ Hz), 78.63 (d, α-C of $Cp^{PSeMes2}$, $J = 12.3$ Hz), 82.60 (d, *ipso*-C of $Cp^{PSeMes2}$, $J = 78.8$ Hz), 132.09 (d, *p*-Aryl C of Ph, $J = 10.7$ Hz), 139.70 (d, *m*-Aryl C of Ph, $J = 3.0$ Hz), 140.49 (brs, *ipso*-C of Mes). ^{31}P {^{1}H} NMR (toluene-d8): δ 19.9 (s, *P*SeMes$_2$, $^1J_{P-Se} = 723$ Hz), 78.5 (s, *P*Se^{t}Bu$_2$, $^1J_{P-Se} = 728$ Hz). ^{77}Se NMR (toluene-d8): δ −71.1 (d, P*Se*Mes$_2$, $^1J_{P-Se} = 721$ Hz), −378.8 (s, P*Se*^{t}Bu$_2$, $^1J_{P-Se} = 728$ Hz). HRMS (APCI-DIP; m/z): $[M]^+$ calc for $C_{36}H_{48}FeP_2Se_2$, 758.091; found 758.061. Anal. Calcd. for $C_{36}H_{48}FeP_2Se_2$: C, 57.16; H, 6.40. Found: C 57.24; H, 6.33.

Copper complexes of ligands 1–3

A suspension of phosphane ligand (**1**, **2** or **3**; 1 mmol) and Cu–C≡C–Ph (1 mmol, 0.165 g for **1** and **2**; 0.5 mmol, 0.083 g for **3**) in a mixture of toluene (19 mL) and thf (1 mL) was heated at 70 °C for 24 h. The resulting hot (~60 °C) solution was quickly filtered through a sintered glass frit (category P4, Pore size 10–16 μm), fitted in a Schlenk filtration apparatus. Over standing the clear filtrate at low temperature (-20 °C) or via a slow diffusion of pentane (~20 mL), amorphous precipitate was obtained, which, after removal of supernant solution, was washed with pentane (~2 mL) and subsequently dried under high vacuum (10^{-3} mbar) for 24 h. NOTE: These complexes, being static in nature, use of an anti-static brush is recommended while working with them. Even after careful handling, the collected yields of these complexes bear substantial procedural loses and thereafter, vary in a range of 40–50 %.

Fc′(PMes$_2$)$_2$·Cu–C≡C–Ph (5)

Yield: 43 %. ^{1}H NMR (solid state): δ −20 to 20 (brm). ^{13}C NMR (solid state): δ 10 to 30 (brm, CH_3^{Mes}), 60 to 85 (brm, C_5H_4), 120 to 150 (brm, C_{aryl}). ^{31}P {^{1}H} NMR (solid state): δ −36 (brs, $PMes_2$). IR (ATR) ν: 1025 (m), 1159 (m), 1440 (m), 1481 (m), 1595 (s), 1929 (s, Stretch for C≡C), 2918 (w). HRMS (MALDI; m/z): $[M]^+$ calc for $C_{46}H_{52}CuFeP_2$, 785.2190; found 785.2189. Anal. Calcd. for $C_{54}H_{57}CuFeP_2$: C, 73.09; H, 6.47; Found: C 72.85; H, 6.57.

Fc′(PMes$_2$)(P^{t}Bu$_2$)·Cu–C≡C–Ph (6)

Yield: 47 %. ^{1}H NMR (solid state): δ −15 to 20 (brm). ^{13}C NMR (solid state): δ 15 to 35 (brm, CH_3^{Mes} and CH_3^{tBu}), 65 to 85 (brm, C_5H_4), 120 to 150 (brm, C_{aryl}). ^{31}P {^{1}H} NMR (solid state): δ −39 (brs, $PMes_2$), 23 (brs, P^tBu_2). IR (ATR) ν: 1026 (m), 1069 (s), 1156 (s), 1440 (m), 1481 (m), 1570 (s), 1594 (s), 1929 (s, broad, Stretch for C≡C), 3047 (w). HRMS (MALDI; m/z): $[M]^+$ calc for $C_{36}H_{48}CuFeP_2$, 661.1877; found 661.1877. Anal. Calcd. for $C_{44}H_{53}CuFeP_2$: C, 69.24; H, 7.00; Found: C 68.94; H, 6.82.

[Fc′(PMes$_2$)Br]·(Cu–C≡C–Ph)$_{0.5}$ (7)

Yield: 48 %. ^{1}H NMR (solid state): δ −13 to 25 (brm). ^{13}C NMR (solid state): δ 15 to 30 (brm, CH_3), 60 to 90 (brm, C_5H_4), 120 to 150 (brm, C_{aryl}). ^{31}P {^{1}H} NMR (solid state): δ −36, −38 (brd, $PMes_2$). IR (ATR) ν: 1085 (s), 1214 (s), 1454 (m), 1496 (m), 1581 (s), 1910 (s, broad, Stretch for C≡C), 3037 (w). NOTE: Despite several attempts of MALDI measurement from a toluene suspension of complex **7**, only the corresponding peak of ligand **3** was found. Due to its poor solubility in common organic solvents, ESI could not be performed. The solid state APCI, being a much harsher ionization technique, could also result in dissociation of the molecule and showed corresponding peaks for **3** ($[M]^+$ at 533) and its oxidized version [Fc′($POMes_2$)Br] ($[M]^+$ at 549). However, the purity of this compound can further be manifested by elemental analysis. Anal. Calcd. for $C_{64}H_{65}Br_2CuFe_2P_2$: C, 62.43; H, 5.32; Found: C 62.69; H, 5.33.

Deposition Numbers 2119545 (for **1**), 2119544 (for **2**), and 2119546 (for **4**) contain the supplementary crystallographic data for this paper. These data are provided free of charge by the joint Cambridge Crystallographic Data Centre and Fachinformationszentrum Karlsruhe Access Structures service www.ccdc.cam.ac.uk/structures.

Author Contributions

Supervision, editing and funding acquisition, R.P. and T.G.; conceptualization, synthesis and characterization of **1**–**7**, writing, and visualization, S.D.; UV-Vis Spectroscopy and electrochemical characterization, F.R., solid-state NMR measurements, M.H., crystallographic structure optimization, C.B. All authors have read and agreed to the published version of the manuscript.

Acknowledgements

RP, SD and FR acknowledge funding by the program MASH from the University of Kassel and the project SMolBits within the LOEWE program of the federal state of Hesse. TG thanks the DFG under contract GU 1650/3-1 for financial support. We thank Prof. Buntkowsky (TU Darmstadt) for generous allocation of measurement time on his 300 MHz Bruker Avance III HD spectrometer. Open Access funding enabled and organized by Projekt DEAL.

Conflict of Interest

The authors declare no conflict of interest.

Data Availability Statement

The data that support the findings of this study are available in the supplementary material of this article.

Keywords: Dppf analogs · Ferrocene · Luminescence · Phosphorus ligand · Solid state nmr

[1] a) S. Dey, R. Pietschnig, *Coord. Chem. Rev.* **2021**, *437*, 213850; b) K. S. Gan, T. S. A. Hor, in *Ferrocenes: Homogeneous Catalysis, Organic Synthesis, Materials Science* (Eds.: A. Togni, T. Hayashi), John Wiley & Sons, **2008**, p. 3; c) G. Bandoli, A. Dolmella, *Coord. Chem. Rev.* **2000**, *209*, 161.

[2] a) M. Trivedi, R. Nagarajan, A. Kumar, N. P. Rath, P. Valerga, *Inorg. Chim. Acta* **2011**, *376*, 549; b) S. Dey, D. Buzsaki, C. Bruhn, Z. Kelemen, R. Pietschnig, *Dalton Trans.* **2020**, *49*, 6668.

[3] M. Trivedi, S. K. Ujjain, G. Singh, A. Kumar, S. K. Dubey, N. P. Rath, *J. Organomet. Chem.* **2014**, *772*, 202.

[4] O. Satoru, M. Atushi, T. Shigeru, *Chem. Lett.* **1989**, *18*, 2037.

[5] T. S. A. Hor, S. P. Neo, C. S. Tan, T. C. W. Mak, K. W. P. Leung, R. J. Wang, *Inorg. Chem.* **1992**, *31*, 4510.

[6] a) L. E. Hagopian, A. N. Campbell, J. A. Golen, A. L. Rheingold, C. Nataro, *J. Organomet. Chem.* **2006**, *691*, 4890; b) T. J. Colacot, S. Parisel, in *Ferrocenes: Ligands, Materials and Biomolecules* (Ed.: P. Štěpnička), John Wiley & Sons, **2008**, p. 117; c) P. Vosáhlo, I. Císařová, P. Štěpnička, *J. Organomet. Chem.* **2018**, *860*, 14; d) A. L. Boyes, I. R. Butler, S. C. Quayle, *Tetrahedron Lett.* **1998**, *39*, 7763; e) W. R. Cullen, T. J. Kim, F. W. B. Einstein, T. Jones, *Organometallics* **1983**, *2*, 714; f) B. C. Hamann, J. F. Hartwig, *J. Am. Chem. Soc.* **1998**, *120*, 3694; g) O. V. Gusev, T. y. A. Peganova, A. M. Kalsin, N. V. Vologdin, P. V. Petrovskii, K. A. Lyssenko, A. V. Tsvetkov, I. P. Beletskaya, *Organometallics* **2006**, *25*, 2750; h) I. R. Butler, W. R. Cullen, T. J. Kim, S. J. Rettig, J. Trotter, *Organometallics* **1985**, *4*, 972; i) T.-Y. Dong, C.-K. Chang, *J. Chin. Chem. Soc.* **1998**, *45*, 577; j) A. Fihri, J.-C. Hierso, A. Vion, D. H. Nguyen, M. Urrutigoïty, P. Kalck, R. Amardeil, P. Meunier, *Adv. Synth. Catal.* **2005**, *347*, 1198; k) M. Yamashita, J. V. Cuevas Vicario, J. F. Hartwig, *J. Am. Chem. Soc.* **2003**, *125*, 16347; l) J.-C. Hierso, F. Lacassin, R. Broussier, R. Amardeil, P. Meunier, *J. Organomet. Chem.* **2004**, *689*, 766; m) M. Laly, R. Broussier, B. Gautheron, *Tetrahedron Lett.* **2000**, *41*, 1183.

[7] a) S. W. Chien, T. S. A. Hor, in *Ferrocenes: Ligands, Materials and Biomolecules* (Ed.: P. Štepnicka), **2008**, p. 33; b) A. Fihri, P. Meunier, J.-C. Hierso, *Coord. Chem. Rev.* **2007**, *251*, 2017.

[8] a) T. J. Colacot, H. A. Shea, *Org. Lett.* **2004**, *6*, 3731; b) G. A. Grasa, T. J. Colacot, *Org. Lett.* **2007**, *9*, 5489.

[9] a) T. R. Kegl, N. Palinkas, L. Kollar, T. Kegl, *Molecules* **2018**, *23*, 3176; b) G. Cavinato, L. Toniolo, *Molecules* **2014**, *19*, 15116.

[10] a) S. Evariste, C. Xu, G. Calvez, C. Lescop, *Inorg. Chim. Acta* **2021**, *516*, 120115; b) C. Lescop, *Chem. Rec.* **2021**, *21*, 544; c) A. M. Khalil, C. Xu, V. Delmas, G. Calvez, K. Costuas, M. Haouas, C. Lescop, *Inorg. Chem. Front.* **2021**, *8*, 4887; d) F. Moutier, J. Schiller, G. Calvez, C. Lescop, *Org. Chem. Front.* **2021**, *8*, 2893; e) M. El Sayed Moussa, A. M. Khalil, S. Evariste, H.-L. Wong, V. Delmas, B. Le Guennic, G. Calvez, K. Costuas, V. W.-W. Yam, C. Lescop, *Inorg. Chem. Front.* **2020**, *7*, 1334; f) S. Evariste, A. M. Khalil, S. Kerneis, C. Xu, G. Calvez, K. Costuas, C. Lescop, *Inorg. Chem. Front.* **2020**, *7*, 3402; g) S. Evariste, M. El Sayed Moussa, H.-L. Wong, G. Calvez, V. W.-W. Yam, C. Lescop, *Z. Anorg. Allg. Chem.* **2020**, *646*, 754; h) S. Evariste, A. M. Khalil, M. E. Moussa, A. K.-W. Chan, E. Y.-H. Hong, H.-L. Wong, B. Le Guennic, G. Calvez, K. Costuas, V. W.-W. Yam, C. Lescop, *J. Am. Chem. Soc.* **2018**, *140*, 12521; i) F. Moutier, A. M. Khalil, S. A. Baudron, C. Lescop, *Chem. Commun.* **2020**, *56*, 10501; j) P. Roesch, J. Nitsch, M. Lutz, J. Wiecko, A. Steffen, C. Müller, *Inorg. Chem.* **2014**, *53*, 9855; k) I. O. Koshevoy, M. Krause, A. Klein, *Coord. Chem. Rev.* **2020**, *405*, 213094; l) I. S. Kritchenkov, A. Y. Gitlina, I. O. Koshevoy, A. S. Melnikov, S. P. Tunik, *Eur. J. Inorg. Chem.* **2018**, *2018*, 3822; m) A. Belyaev, T. Eskelinen, T. M. Dau, Y. Y. Ershova, S. P. Tunik, A. S. Melnikov, P. Hirva, I. O. Koshevoy, *Chem. Eur. J.* **2018**, *24*, 1404; n) R. R. Ramazanov, A. I. Kononov, A. M. Nesterenko, J. R. Shakirova, I. O. Koshevoy, E. V. Grachova, S. P. Tunik, *J. Phys. Chem. C* **2016**, *120*, 25541; o) T. M. Dau, B. D. Asamoah, A. Belyaev, G. Chakkaradhari, P. Hirva, J. Jänis, E. V. Grachova, S. P. Tunik, I. O. Koshevoy, *Dalton Trans.* **2016**, *45*, 14160; p) I. S. Krytchankou, I. O. Koshevoy, V. V. Gurzhiy, V. A. Pomogaev, S. P. Tunik, *Inorg. Chem.* **2015**, *54*, 8288; q) S. Perruchas, *Dalton Trans.* **2021**, *50*, 12031; r) Q. Benito, N. Desboeufs, A. Fargues, A. Garcia, F. Massuyeau, C. Martineau-Corcos, T. Devic, S. Perruchas, *New J. Chem.* **2020**, *44*, 19850; s) R. Utrera-Melero, B. Huitorel, M. Cordier, J.-Y. Mevellec, F. Massuyeau, C. Latouche, C. Martineau-Corcos, S. Perruchas, *Inorg. Chem.* **2020**, *59*, 13607; t) R. Utrera-Melero, J.-Y. Mevellec, N. Gautier, N. Stephant, F. Massuyeau, S. Perruchas, *Chem. Asian J.* **2019**, *14*, 3166; u) B. Huitorel, R. Utrera-Melero, F. Massuyeau, J.-Y. Mevelec, B. Baptiste, A. Polian, T. Gacoin, C. Martineau-Corcos, S. Perruchas, *Dalton Trans.* **2019**, *48*, 7899; v) J. Nitsch, C. Kleeberg, R. Fröhlich, A. Steffen, *Dalton Trans.* **2015**, *44*, 6944; w) C. Kutal, *Coord. Chem. Rev.* **1990**, *99*, 213; x) R. D. Pike, K. E. deKrafft, A. N. Ley, T. A. Tronic, *Chem. Commun.* **2007**, 3732; y) W.-F. Fu, X. Gan, C.-M. Che, Q.-Y. Cao, Z.-Y. Zhou, N. N.-Y. Zhu, *Chem. Eur. J.* **2004**, *10*, 2228; z) X.-Y. Chang, K.-H. Low, J.-Y. Wang, J.-S. Huang, C.-M. Che, *Angew. Chem. Int. Ed.* **2016**, *55*, 10312.

[11] a) M. N. Chevykalova, *Russ. Chem. Bull.* **2003**, *52*, 78; b) A. Orthaber, M. Fuchs, F. Belaj, G. N. Rechberger, C. O. Kappe, R. Pietschnig, *Eur. J. Inorg. Chem.* **2011**, *2011*, 2588.

[12] a) B. Milde, M. Lohan, C. Schreiner, T. Rüffer, H. Lang, *Eur. J. Inorg. Chem.* **2011**, *2011*, 5437–5449; b) R. P. Pinnell, C. A. Megerle, S. L. Manatt, P. A. Kroon, *J. Am. Chem. Soc.* **1973**, *95*, 977.

[13] a) D. W. Allen, B. F. Taylor, *J. Chem. Soc. Dalton Trans.* **1982**, 51; b) B. A. Demko, K. Eichele, R. E. Wasylishen, *J. Phys. Chem. A* **2006**, *110*, 13537; c) C. G. Hrib, F. Ruthe, E. Seppälä, M. Bätcher, C. Druckenbrodt, C. Wismach, P. G. Jones, W.-W. du Mont, V. Lippolis, F. A. Devillanova, M. Bühl, *Eur. J. Inorg. Chem.* **2006**, *2006*, 88–100.

[14] R. García-Rodríguez, H. Liu, *J. Am. Chem. Soc.* **2012**, *134*, 1400–1403.

[15] a) C. A. Tolman, *Chem. Rev.* **2002**, *77*, 313; b) R. Starosta, B. Bażanów, W. Barszczewski, *Dalton Trans.* **2010**, *39*, 7547.

[16] S. Isenberg, S. Weller, D. Kargin, S. Valic, B. Schwederski, Z. Kelemen, C. Bruhn, K. Krekic, M. Maurer, C. M. Feil, M. Nieger, D. Gudat, L. Nyulaszi, R. Pietschnig, *Chem. Open* **2019**, *8*, 1235.

[17] a) A. Lik, D. Kargin, S. Isenberg, Z. Kelemen, R. Pietschnig, H. Helten, *Chem. Commun.* **2018**, *54*, 2471; b) D. Kargin, Z. Kelemen, K. Krekic, M. Maurer, C. Bruhn, L. Nyulaszi, R. Pietschnig, *Dalton Trans.* **2016**, *45*, 2180; c) S. Borucki, Z. Kelemen, M. Maurer, C. Bruhn, L. Nyulászi, R. Pietschnig, *Chem. Eur. J.* **2017**, *23*, 10438.

[18] a) J. Díez, M. P. Gamasa, J. Gimeno, A. Aguirre, S. García-Granda, J. Holubova, L. R. Falvello, *Organometallics* **1999**, *18*, 662; b) M. Trivedi, G. Singh, A. Kumar, N. P. Rath, *Dalton Trans.* **2015**, *44*, 20874; c) P. C. Ford, E. Cariati, J. Bourassa, *Chem. Rev.* **1999**, *99*, 3625; d) L. Naldini, F. Demartin, M. Manassero, M. Sansoni, G. Rassu, M. A. Zoroddu, *J. Organomet. Chem.* **1985**, *279*, c42; e) V. W.-W. Yam, W.-K. Lee, K.-K. Cheung, B. Crystall, D. Phillips, *J. Chem. Soc. Dalton Trans.* **1996**, 3283; f) A. Belyaev, T. M. Dau, J. Jänis, E. V. Grachova, S. P. Tunik, I. O. Koshevoy, *Organometallics* **2016**, *35*, 3763.

[19] a) S. S. Chui, M. F. Ng, C. M. Che, *Chem. Eur. J.* **2005**, *11*, 1739; b) V. W.-W. Yam, W. K.-M. Fung, K.-K. Cheung, *Chem. Commun.* **1997**, 963; c) A. Y. Baranov, E. A. Pritchina, A. S. Berezin, D. G. Samsonenko, V. P. Fedin, N. A. Belogorlova, N. P. Gritsan, A. V. Artem'ev, *Angew. Chem. Int. Ed.* **2021**, *60*, 12577.

[20] M. Trivedi, G. Singh, A. Kumar, N. P. Rath, *Dalton Trans.* **2014**, *43*, 13620.

[21] a) A. Grünberg, T. Gutmann, N. Rothermel, X. Yeping, H. Breitzke, G. Buntkowsky, *Z. Phys. Chem.* **2013**, *227*, 901; b) A. Grünberg, X. Yeping, H. Breitzke, G. Buntkowsky, *Chem. Eur. J.* **2010**, *16*, 6993.

[22] a) C. R. Bock, E. A. K. Von Gustorf, in *Adv. Photochem.*, John Wiley & Sons, **1977**, p. 221; b) G. B. Maiya, J. M. Barbe, K. M. Kadish, *Inorg. Chem.* **1989**, *28*, 2524; c) A. Vogler, H. Kunkely, in *Photosensitization and Photocatalysis Using Inorganic and Organometallic Compounds* (Eds.: K. Kalyanasundaram, M. Grätzel), Springer Netherlands, Dordrecht, **1993**, p. 71; d) P. D. Beer, F. Szemes, V. Balzani, C. M. Salà, M. G. B. Drew, S. W. Dent, M. Maestri, *J. Am. Chem. Soc.* **1997**, *119*, 11864; e) B. Delavaux-Nicot, S. Fery-Forgues, *Eur. J. Inorg. Chem.* **1999**, *1999*, 1821; f) S. Fery-Forgues, B. Delavaux-Nicot, *J. Photochem. Photobiol. A* **2000**, *132*, 137; g) R. Giasson, E. J. Lee, X. Zhao, M. S. Wrighton, *J. Phys. Chem.* **2002**, *97*, 2596; h) J. Maynadié, B. Delavaux-Nicot, S. Fery-Forgues, D. Lavabre, R. Mathieu, *Inorg. Chem.* **2002**, *41*, 5002; i) S. K. Gibbons, R. P. Hughes, D. S. Glueck, A. T. Royappa, A. L. Rheingold, R. B. Arthur, A. D. Nicholas, H. H. Patterson, *Inorg. Chem.* **2017**, *56*, 12809.

[23] X. Wu, W. Zhang, X. Zhang, N. Ding, T. S. A. Hor, *Eur. J. Inorg. Chem.* **2015**, *2015*, 876.

[24] V. K. K. Pampana, A. Sagadevan, A. Ragupathi, K. C. Hwang, *Green Chem.* **2020**, *22*, 1164.

[25] G. R. Fulmer, A. J. M. Miller, N. H. Sherden, H. E. Gottlieb, A. Nudelman, B. M. Stoltz, J. E. Bercaw, K. I. Goldberg, *Organometallics* **2010**, *29*, 2176.

Research Article
doi.org/10.1002/ejic.202100939

[26] A. E. Bennett, C. M. Rienstra, M. Auger, K. V. Lakshmi, R. G. Griffin, *J. Chem. Phys.* **1995**, *103*, 6951.
[27] G. M. Sheldrick, *Acta Crystallogr. Sect. A* **2008**, *64*, 112.
[28] a) C. F. Macrae, I. J. Bruno, J. A. Chisholm, P. R. Edgington, P. McCabe, E. Pidcock, L. Rodriguez-Monge, R. Taylor, J. van de Streek, P. A. Wood, *J. Appl. Crystallogr.* **2008**, *41*, 466; b) C. F. Macrae, P. R. Edgington, P. McCabe, E. Pidcock, G. P. Shields, R. Taylor, M. Towler, J. van de Streek, *J. Appl. Crystallogr.* **2006**, *39*, 453; c) A. L. Spek, *Acta Crystallogr. Sect. C* **2015**, *71*, 9.
[29] I. Noviandri, K. N. Brown, D. S. Fleming, P. T. Gulyas, P. A. Lay, A. F. Masters, L. Phillips, *J. Phys. Chem. B* **1999**, *103*, 6713.

Manuscript received: November 1, 2021
Revised manuscript received: November 30, 2021
Accepted manuscript online: December 3, 2021